

DOI: <https://doi.org/10.37434/tpwj2026.05.01>

# FORMATION OF COATINGS CONTAINING MAX-PHASES UNDER THERMAL SPRAYING CONDITIONS OF TiC–TiH<sub>2</sub>–Al POWDER

N.V. Vihilianska<sup>1</sup>, T.V. Tsymbalista<sup>1</sup>, O.P. Gryshchenko<sup>1</sup>, I.O. Koziakov<sup>1</sup>, O.Y. Gudymenko<sup>2</sup>

<sup>1</sup>E.O. Paton Electric Welding Institute of the NASU  
11 Kazymyr Malevych Str., 03150, Kyiv, Ukraine

<sup>2</sup>V.E. Lashkaryov Institute of Semiconductor Physics of the NASU  
45 Prosp. Nauky, 02000, Kyiv, Ukraine

## ABSTRACT

The study investigates the formation of coatings via plasma spraying (PS) and high-velocity oxyfuel spraying (HVOF) using a TiH<sub>2</sub>–Al–TiC powder system. The composite powder was obtained by processing a powder mixture of the initial components TiH<sub>2</sub>, Al and TiC in a planetary mill for 5 h, resulting in the formation of agglomerated particles with a size of <40 μm. The resulting composite powder contains the initial components of the mixture and the products of their interaction — titanium aluminide Ti<sub>3</sub>Al, and MAX-phase carbide (Ti<sub>3</sub>AlC, Ti<sub>2</sub>AlC). The coatings, produced by plasma and high-velocity oxyfuel spraying methods, were investigated using X-ray phase analysis, optical microscopy and microhardness testing. It has been established that during plasma spraying, the phase composition of the produced coating differs significantly from that of the MChS powder used for spraying. The coating retains a TiC phase, but in a smaller quantity than in the initial powder, and contains a TiCN phase, which was formed during the interaction of nitrogen atoms with TiC as the powder passed through the plasma jet of powder particles and came into contact with the gaseous medium. Peaks for Al, the MAX-phase of Ti<sub>2</sub>AlC and Ti<sub>3</sub>AlC carbide were not detected in the X-ray diffraction pattern, which is likely associated with the intense oxidation of the powder particles, resulting in the formation of titanium oxide TiO<sub>2</sub> in two forms (rutile and anatase) and aluminium oxide Al<sub>2</sub>O<sub>3</sub>. The coating contains Ti<sub>3</sub>Al and TiH<sub>2</sub> phases in negligible amounts, which are present in the initial MChS powder. The plasma coating has a lamellar light structure with voids in the form of spalling (11 %) and contains unmelted fine powder particles. In high-velocity oxyfuel spraying, the phase composition of the coating differs only slightly from that of the initial powder; the coating inherits the phase composition of the initial MChS powder, as no new compounds are formed apart from oxides. The coating structure is thin-lamellar, consisting of light-coloured metallic and grey oxide layers, with a small amount of unmelted particles and a porosity of (~2 %). The microhardness of TiC–TiH<sub>2</sub>–Al system coatings is 5400±1060 MPa for the PS coating and 3710±950 MPa for the HVOF coating.

**KEYWORDS:** coatings, plasma spraying, high-velocity oxyfuel spraying, MAX-phase, mechanochemical synthesis, phase composition, structure, microhardness

## INTRODUCTION

The ternary compounds Ti<sub>3</sub>AlC<sub>2</sub> and Ti<sub>2</sub>AlC belong to a leading group of ceramic materials known as MAX-phases. These phases are damage-resistant and combine ceramic and metallic properties. Like metals, they are thermally and electrically conductive, can be easily machined using conventional tools, and are resistant to thermal shocks. As ceramics, Ti<sub>3</sub>AlC<sub>2</sub> and Ti<sub>2</sub>AlC are lightweight, elastic-rigid and thermally stable, and retain their strength at high temperatures, forming a continuous Al<sub>2</sub>O<sub>3</sub> oxide layer on the surface of Ti<sub>3</sub>AlC<sub>2</sub> and Ti<sub>2</sub>AlC at high temperatures. In particular, Ti<sub>3</sub>AlC<sub>2</sub> exhibits some anomalous compressive ductility at room temperature compared to conventional ceramics. Due to this unusual combination of properties, Ti<sub>3</sub>AlC<sub>2</sub> and Ti<sub>2</sub>AlC are considered potentially attractive materials for various functional and structural applications, such as: structural materials for high temperatures, heat exchangers for nuclear power plants, and materials for electrical contacts [1].

The synthesis of the Ti<sub>3</sub>AlC<sub>2</sub> MAX-phase was first described in 1994 by Pitzka and Schuster by sintering powder mixtures of Ti, TiAl, Al<sub>4</sub>C<sub>3</sub> and C [2]. The most widely used combinations of initial materials for producing the Ti<sub>3</sub>AlC<sub>2</sub> MAX-phase are Ti/Al<sub>4</sub>C<sub>3</sub>/C, Ti/Al/C, Ti/Al<sub>4</sub>C<sub>3</sub>/TiC, Ti/Al/TiC, and Ti/Al/C/TiC [3, 4]. However, Ti<sub>3</sub>AlC is very difficult to synthesize due to its rather narrow phase range on the Ti–Al–C ternary phase diagram [2].

In most methods, metal powders have been used as the source of Ti; these are expensive and result in a high cost for Ti<sub>3</sub>AlC<sub>2</sub> [4]. TiH<sub>2</sub> powders are intermediate products in the production of Ti metal powders and are cheaper than Ti powders. The cost of TiH<sub>2</sub> powders is 10 % lower than that of Ti powders with equivalent particle sizes. Nevertheless, when TiH<sub>2</sub> powders are used to produce Ti<sub>3</sub>AlC<sub>2</sub>, a prolonged annealing time is essential to remove hydrogen from the TiH<sub>2</sub> prior to sintering. Furthermore, this dehydrogenation process causes the formation of numerous pores in the synthesized products. Auxiliary pressure

is required during sintering to compact the samples. Increased cost due to expensive treatment is compensated by reduced cost due to cheaper raw materials. Therefore, the use of  $\text{TiH}_2$  instead of Ti is appropriate for the production of powders, rather than dense  $\text{Ti}_3\text{AlC}_2$  specimens.

When using  $\text{TiH}_2$  as a source of Ti for the synthesis of the  $\text{Ti}_3\text{AlC}_2$  MAX-phase, combinations of  $\text{TiH}_2/\text{Al}/\text{TiC}$  [4–8],  $\text{TiH}_2/\text{Al}/\text{C}$  [9–12] and  $\text{TiC}/\text{TiH}_2/\text{Al}/\text{C}$  [13] powders are used. For the synthesis of the  $\text{Ti}_3\text{AlC}_2$  MAX-phase, the powders were sintered in a vacuum using the pulse discharge sintering (PDS) method (PAS-V, Sodick Co. Ltd.) (so-called SPS) [4, 9], the powders were sintered in a tube furnace in an argon atmosphere using the pressureless reactive sintering (PLS) method [5], synthesis of powders in a vacuum furnace in an argon atmosphere [6–8], and the reactive synthesis method [10, 11], microwave sintering (MWS) [12], and self-propagating high-temperature synthesis (SHS) [13].

The pulsed discharge sintering (PDS) method, also known as spark plasma sintering (SPS), is a recent innovation; its versatility allows for rapid densification to near-theoretical density in a range of metallic, ceramic and other engineering components. During sintering using the PDS method in a  $\text{TiH}_2/\text{Al}/\text{TiC}$  powder mixture [4], it was found that the synthesis mechanism of  $\text{Ti}_3\text{AlC}_2$  occurs via reactions between the intermediate phases  $\text{AlTi}_3$ ,  $\text{Al}_3\text{Ti}$ ,  $\text{AlTi}$  and  $\text{Ti}_2\text{AlC}$ , as well as the initial reagents.

During PLS sintering [5], 95 wt.% pure  $\text{Ti}_3\text{AlC}_2$  was produced from a  $\text{TiH}_2/\text{Al}/\text{TiC}$  powder mixture; the sample had a porous structure and easily crumbled into powder. When adding Sn or Si to  $\text{TiH}_2/\text{Al}/\text{TiC}$ , the synthesis temperature decreased to 1200 °C, and a single-phase  $\text{Ti}_3\text{AlC}_2$  product was obtained with a compact, almost pore-free microstructure.

After the synthesis of  $\text{TiH}_2/\text{Al}/\text{TiC}$  powders in a vacuum furnace in an argon atmosphere [6–8], the phase composition of the samples after synthesis was found to be: 92 %  $\text{Ti}_3\text{AlC}_2$  and 8 %  $\text{Al}_2\text{O}_3$  [6], 91.51 %  $\text{Ti}_3\text{AlC}_2$  and 8.49 %  $\text{Al}_2\text{O}_3$  with a porosity of 13 % [7], 95 %  $\text{Ti}_3\text{AlC}_2$  and 5 % TiC with a porosity of 22 %; after hot pressing, the grains were significantly refined and the pore size decreased to 1 %, whilst the phase composition contained 89 %  $\text{Ti}_3\text{AlC}_2$ ; 6 % TiC; 5 %  $\text{Al}_2\text{O}_3$  [8].

During the PDS sintering of a  $\text{TiH}_2/\text{Al}/\text{C}$  powder mixture [9], the dehydrogenation reaction was not complete when the powders were heated to 900 °C; compared with the  $\text{TiH}_2/\text{Al}/\text{TiC}$  powder mixture [4], the content of the  $\text{Ti}_3\text{AlC}_2$  phase in the  $\text{TiH}_2/\text{Al}/\text{C}$  mixture was low. This can be explained by the greater amount of  $\text{TiH}_2$  powder used in the initial powders

than in the case of the  $\text{TiH}_2/\text{Al}/\text{TiC}$  powder mixture [4], in which approximately two-thirds of the Ti originated from TiC.

Porous ceramics with a 100 %  $\text{Ti}_3\text{AlC}_2$  content were successfully produced by reactive synthesis [10, 11] using  $\text{TiH}_2/\text{Al}/\text{C}$  with varying Al content in the powder mixture. The effect of varying Al content on the phase composition of the powder mixture and on the pore structure was systematically investigated in the powder mixture [11], which showed that single-phase porous  $\text{Ti}_3\text{AlC}_2$  ceramics can be obtained by adjusting the amount of aluminium. As the Al content increases, the weight percentage of the  $\text{Ti}_3\text{AlC}_2$  MAX-phase grows, as well as the open and total porosity; the maximum porosity is observed at 100 %  $\text{Ti}_3\text{AlC}_2$  content.

During sintering by the MWS method [12], the synthesis reaction of  $\text{Ti}_3\text{AlC}_2$  in the  $\text{TiH}_2/\text{Al}/\text{C}$  powder mixture occurs at lower temperatures unlike with other sintering methods.

In the powder mixture  $2.6\text{Ti} + 1.2\text{Al} + 2\text{C} + 0.1\text{TiH}_2$  [13], the content of  $\text{Ti}_3\text{AlC}_2$  is 80.6 wt.%,  $\text{Ti}_2\text{AlC}$  is 13.6 wt.%, and TiC is 5.8 wt.%. With an increase in  $\text{TiH}_2$ , a decrease in  $\text{Ti}_3\text{AlC}_2$  was observed, accompanied by an increase in  $\text{Ti}_2\text{AlC}$ . In the mixture  $2.6\text{Ti} + 1.2\text{Al} + 2\text{C} + 0.4\text{TiH}_2$ , 67.8 wt.%  $\text{Ti}_3\text{AlC}_2$ , 28.6 wt.%  $\text{Ti}_2\text{AlC}$  and 3.7 wt.% TiC were found. This may be associated with incomplete decomposition of  $\text{TiH}_2$  due to a decrease in combustion temperature with an increase in  $\text{TiH}_2$  content. The thermal decomposition of  $\text{TiH}_2$  was intended to provide Ti for the synthesis reaction. Due to a lack of Ti when  $\text{TiH}_2$  is added, the amount of TiC decreases, which hinders the phase transition from  $\text{Ti}_2\text{AlC}$  to  $\text{Ti}_3\text{AlC}_2$ .

Mechanical grinding, mechanical activation and mechanical synthesis technologies are also successfully used in the production of so-called MAX-phases ( $\text{Mn} + 1\text{AXn}$ ). Among sintering methods, mechanochemical synthesis (MChS) has attracted considerable attention from materials scientists due to the ease of synthesizing supersaturated solid solutions, amorphous phases, intermetallics and nanocrystalline materials in almost all alloys at room temperature. MChS is successfully used for the production of MAX-phases [14–17]. For the Ti–Al–C MChS system, the mixing of powders of titanium (titanium oxide or titanium hydride), aluminium and graphite generally leads to the formation of Ti–Al intermetallic compounds and titanium carbide, whilst MAX-phases are formed in small quantities. MAX-phases of various stoichiometries are predominantly formed during subsequent heat treatment of the powder at 600–1700 °C or during sintering of the powders within this tem-

perature range, due to the interaction of the titanium and aluminium melts with carbide (TiC or Al<sub>4</sub>C<sub>3</sub>).

The PVD deposition method is used to produce thin films containing the Ti<sub>3</sub>AlC<sub>2</sub> MAX-phase [18]. Coatings with a thickness exceeding 100 µm are typically required for applications under high temperatures or severe conditions. Thermal spraying methods are used to deposit coatings with a thickness of >50 µm. The advantages of thermal spraying processes over other deposition methods lie in the simplicity of the equipment, the absence of the need to carry out processes in a shielding atmosphere, and the ability to produce coatings up to several millimetres thick on parts of various configurations. However, popular modern thermal spraying methods, such as plasma arc and high-velocity oxyfuel spraying, have not found widespread application in the formation of Ti<sub>3</sub>AlC<sub>2</sub>-based coatings due to the high flame temperature, which typically causes decomposition and/or oxidation of MAX-phases [19–22]. Instead, the PS and HVOF methods are used to deposit coatings based on the Ti<sub>2</sub>AlC MAX-phase, in which the Ti<sub>3</sub>AlC<sub>2</sub> MAX-phase is formed as a result of phase transformations during the deposition process [21, 22].

Coatings with a high content of the Ti<sub>3</sub>AlC<sub>2</sub> MAX-phase (74–84 %) were produced by a plasma method using a spray material in the form of a suspension [23]. In this case, unlike conventional air-plasma spraying, a liquid stream is used to feed the powder into the heat source instead of a carrier gas. This modification allows omitting the stage of heating the powder with a plasma torch, thereby enabling the deposition of heat-sensitive coatings.

### THE AIM

of the study is to investigate the formation of coatings during plasma and high-velocity oxyfuel spraying of a TiC–TiH<sub>2</sub>–Al composite powder produced by mechanochemical synthesis.

### MATERIALS AND PROCEDURES OF RESEARCH

A composite powder (CP) obtained by the MChS method from a TiC/TiH<sub>2</sub>/Al powder mixture was used as the spraying material. The following powders were used as initial materials for obtaining CP:

- TiC powder (40–63 µm, TU 6-09-492–75) — 79.2–80 Ti, 0.1–0.2 C (free), 19.4–20.2 C (total), 0.1–0.6 Fe;
- titanium dihydride powder TiH<sub>2</sub> (<40 µm, TU U 114-10-026–98) — 0.10 Fe, 0.06 Cl, 0.04 N;
- Al powder (PA-4, –50 + 40 µm) — <0.4 Si, <0.35 Fe, <0.02 Cu.

The composition of initial powders in the mixture was calculated to yield the Ti<sub>3</sub>AlC<sub>2</sub> MAX-phase according to reaction (1) and was 60.9TiC–25.4TiH<sub>2</sub>–13.7Al (wt.%).



The MChS process of the powder mixture was carried out in an Activator 2SL high-energy mill for 5 h at a velocity of 600–900 rpm. Plasma spraying was carried out using a serial UPU-8M installation with a Metco F4 MB plasmatron. For coating spraying using the high-velocity oxyfuel spraying method, a VShGPN-1 installation was used, manufactured at the PWI based on the HIPOJET 2700M prototype (Metallizing Equipment Co. Pvt. Ltd., India). The process parameters for PS and HVOF are given in Tables 1 and 2.

The following methods were used to investigate the powders and sprayed coatings: metallography, microhardness testing and X-ray diffraction phase analysis (XRD). A Neophot-32 optical microscope with a digital photography attachment was used to examine the structure of the powders and sprayed coatings. For quantitative analysis of the pore content in the coatings, an optical method (image analysis method) was employed, which involves determining the area occu-

**Table 1.** Process parameters for PS-coatings using a TiC–TiH<sub>2</sub>–Al powder system

Parameter	Value
Current, A	600
Voltage, V	40
Flow rate of plasma-forming gas Ar/N <sub>2</sub> , l/min	30
Ratio of plasma-forming gas Ar/N <sub>2</sub> , %	80/20
Flow rate of carrier gas N <sub>2</sub> , l/min	5
Powder feed rate, kg/h	1.4
Spray distance, mm	100

**Table 2.** Process parameters for HVOF-coatings using a TiC–TiH<sub>2</sub>–Al powder system

Parameter	Value
CH <sub>4</sub> fuel gas flow rate, l/min	28
CH <sub>4</sub> fuel gas pressure, atm	5.5
Oxygen flow rate, m <sup>3</sup> /h	4
Oxygen pressure, atm	8
Air flow rate, m <sup>3</sup> /h	15
Air pressure, atm	5
Carrier gas flow rate, l/min	20
Carrier gas pressure, atm	5
Spray distance, mm	140

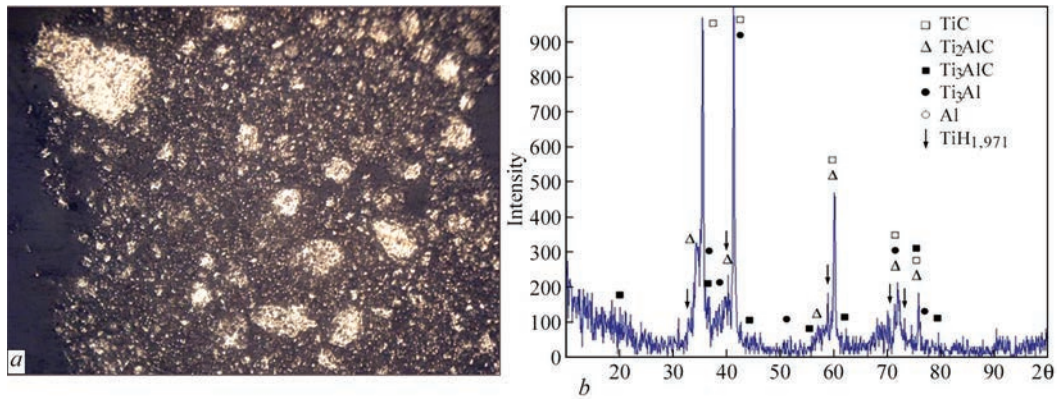


**Figure 1.** Microstructure (a) and X-ray diffraction pattern (b) of the TiC–TiH<sub>2</sub>–Al coating

pied by the detected pores relative to the total area of the coating section. The digital image was processed using Image-Pro Plus software, which enables the measurement of porosity (by identifying inclusions that differ in colour and brightness) and the determination of their number and percentage by area.

The phase composition of the powder particles and the coating was studied using a PANalytical X’Pert PRO X-ray diffractometer with CuK $\alpha$  radiation ( $\lambda = 0.15406$  nm). The anode voltage of the tube was 45 kV, and the current was 40 mA. Diffraction patterns were recorded at 0.025° interval with a sampling time of 1 s per point. The data from the diffractometric measurements were processed using the High Score Plus software.

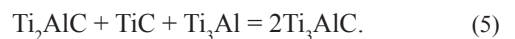
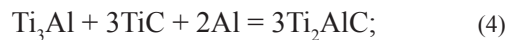
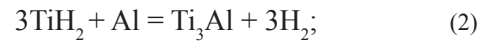
The microhardness of the coatings was investigated using a PMT-3 microhardness tester at a load of 50 g. The principle of operation of the PMT-3 instrument is based on indentation of a diamond pyramid into the tested material under a specific load and measuring the linear dimension of the diagonal of the resulting indentation.

### EXPERIMENTAL RESULTS AND DISCUSSION

The use of aluminium (belongs to a ductile material) as the initial component facilitates the repeated processes of "cold" welding and refinement, resulting in the formation of conglomerated particles with a size

of <40  $\mu\text{m}$  after 5 h of processing at a drum rotation velocity of 900 rpm (Figure 1, a).

X-ray phase analysis has shown (Figure 1, b) that the CP produced after 5 h of processing has a multi-phase structure consisting of the initial components (TiC, TiH<sub>x</sub>, Al) and the products of their mutual interaction, the formation of which may proceed via the following reactions: titanium aluminide Ti<sub>3</sub>Al according to reaction (2), the MAX-phase Ti<sub>2</sub>AlC according to reactions (3) and/or (4), and the ternary compound Ti<sub>3</sub>AlC according to reaction (5).



During the spraying of the TiC–TiH<sub>2</sub>–Al powder system using the PS method, significant phase transformations occur; the phase composition of the produced coating (Figure 2, a) differs significantly from that of the sprayed MChS powder. The coating has a crystalline structure; the TiC phase remains in the coating, but in a smaller quantity than in the initial powder. No peaks of Al, the Ti<sub>2</sub>AlC MAX-phase, or Ti<sub>3</sub>AlC carbide were detected in the X-ray diffraction pattern; this is evidently associated with the intense oxidation of the powder particles, resulting in the formation of titanium oxide TiO<sub>2</sub> in two forms (rutile and

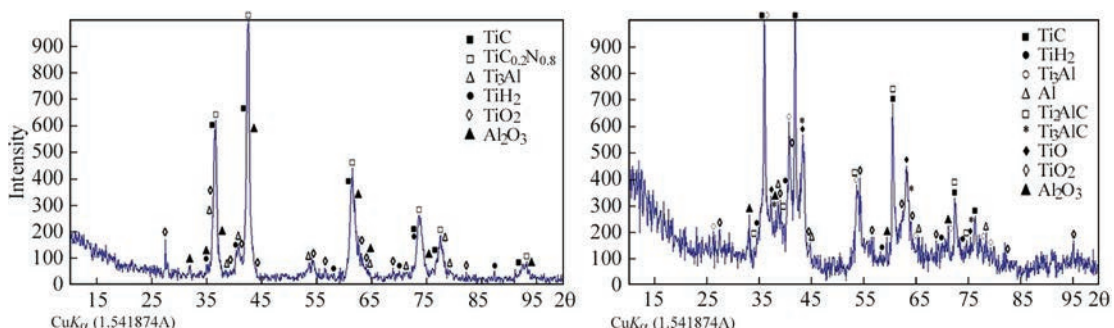
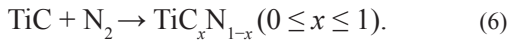


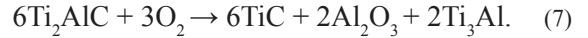
**Figure 2.** X-ray diffraction patterns of coatings produced from TiC–TiH<sub>2</sub>–Al powder: a — PS; b — HVOF

anatase) and aluminium oxide  $\text{Al}_2\text{O}_3$ . The  $\text{Ti}_3\text{Al}$  and  $\text{TiH}_2$  phases, which are present in the initial MChS powder, are present in the coating in negligible quantities. The X-ray diffraction pattern shows peak splitting near the  $\text{TiC}$  peak, which belongs to the  $\text{TiCN}$  phase; the formation of this phase is associated with the interaction of nitrogen atoms with  $\text{TiC}$  as the powder particles pass through the plasma jet, where they come into contact with the gaseous medium during the reaction:

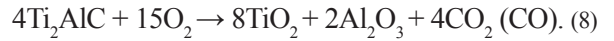


Unlike plasma spraying, in the HVOF process the  $\text{TiC-TiH}_2\text{-Al}$  powder particles do not undergo significant phase transformations, and the phase composition of the coating differs only slightly from that of the powder (Figure 2, *b*). In the coating, as in the MChS powder, the phases  $\text{TiC}$ ,  $\text{Ti}_3\text{Al}$ , as well as the MAX-phase  $\text{Ti}_2\text{AlC}$  and the carbide  $\text{Ti}_3\text{AlC}$  are present; their quantities in the coating are slightly reduced compared to the MChS powder, which is a consequence of the interaction of these components with oxygen during the spraying process, leading to the formation of titanium oxides  $\text{TiO}$ ,  $\text{Ti}_2\text{O}_3$  and aluminium oxide  $\text{Al}_2\text{O}_3$ . Thus, it can be concluded that in HVOF, the coating inherits the phase composition of the initial MChS powder, since no new compounds, apart from oxides, are formed.

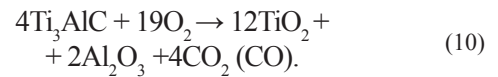
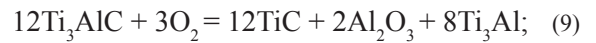
The partial or complete decomposition of the  $\text{Ti}_2\text{AlC}$  MAX-phase during HVOF and plasma spraying of the  $\text{TiC-TiH}_2\text{-Al}$  coating system occurs through the following reactions. At temperatures of 600–1000 °C, partial decomposition of  $\text{Ti}_2\text{AlC}$  takes place, leading to the formation of  $\text{TiC}$ ,  $\text{Al}_2\text{O}_3$  and  $\text{Ti}_3\text{Al}$  phases through the reaction (7).



At temperatures >1000 °C, the MAX-phase structure is destroyed and completely oxidized to  $\text{TiO}_2$ ,  $\text{Al}_2\text{O}_3$  and  $\text{CO}_2/\text{CO}$  according to the reaction (8).



The decomposition of the  $\text{Ti}_3\text{AlC}$  carbide phase proceeds in a similar manner through the following reactions (9), (10).



The  $\text{TiC-TiH}_2\text{-Al}$  plasma coating has a lamellar light-coloured structure with yellow and a few dark brown lamellae (Figure 3, *a*). The coating contains voids in the form of spalling, accounting for 11 % of the volume, formed during the preparation of the coating's microsection as a result of its brittleness. Unmelted fine powder particles are also observed in the coating. In HVOF, coatings with a dense, thin-lamellar

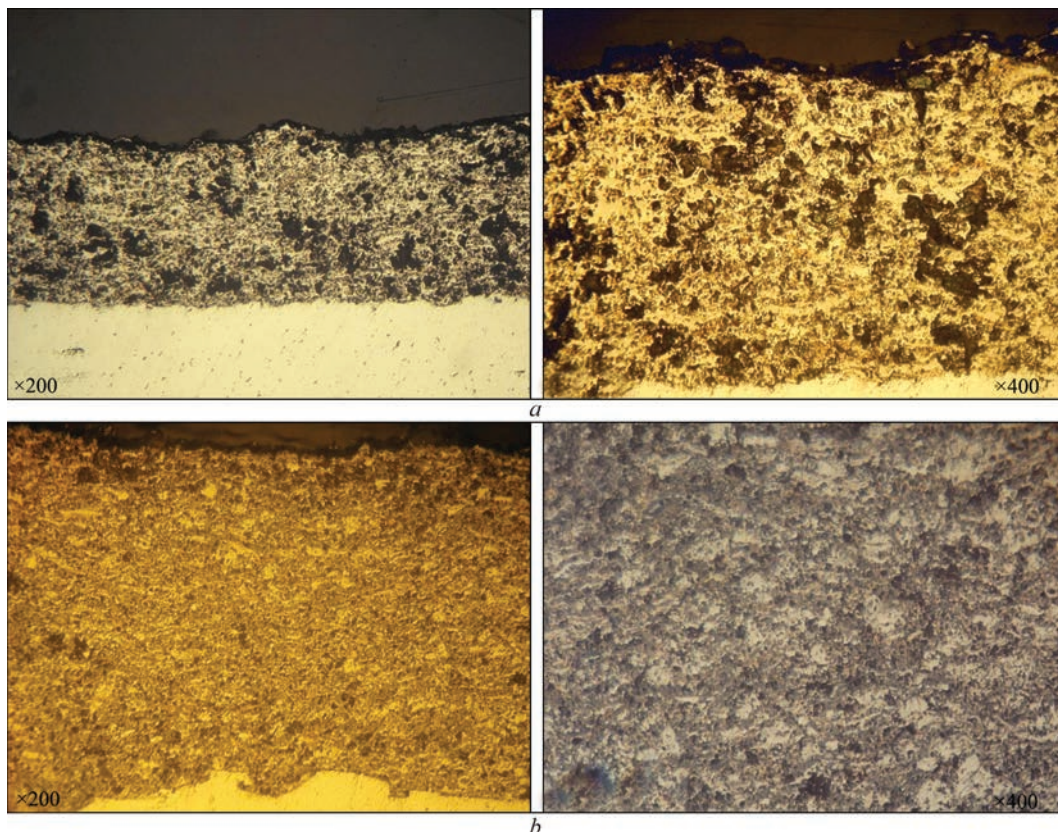
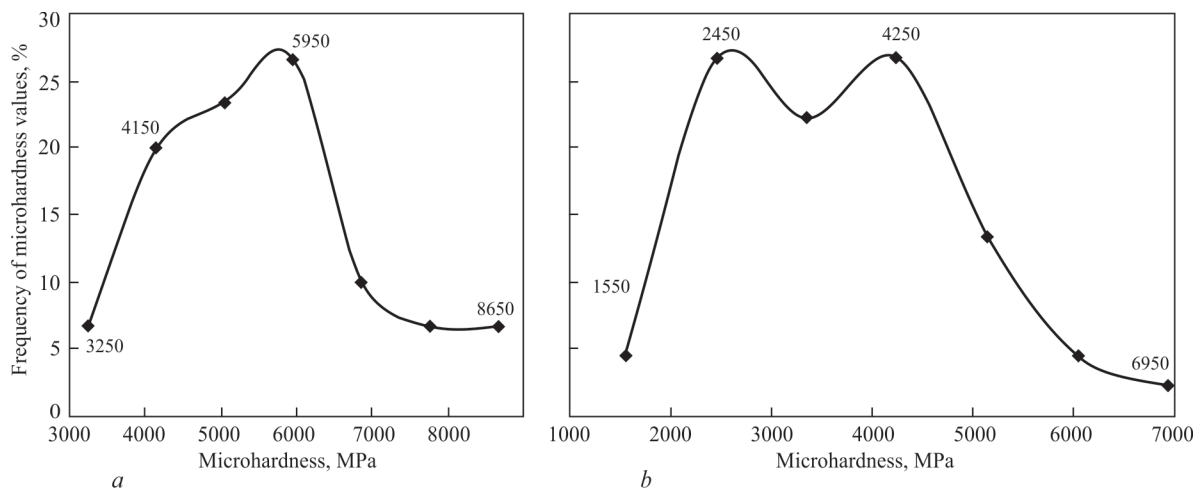


Figure 3. Microstructure of coatings produced from  $\text{TiC-TiH}_2\text{-Al}$  powder: *a* — PS; *b* — HVOF



**Figure 4.** Variation curves of the microhardness distribution of TiC-TiH<sub>2</sub>-Al system coatings produced by PS (a) and HVOF (b) methods

structure are formed, comprising light-coloured metallic and grey oxide interlayers and a small number of unmelted particles (Figures 3, b). The presence of unmelted particles indicates that the powder particles with a higher melting point do not have time to heat up during the short residence time in the jet and, as a result of high-velocity spraying, do not acquire the necessary ductility to form lamellae and are deposited in the coating in a solid or slightly ductile state. The coating has a low porosity (~2 %).

The multiphase nature of the TiC-TiH<sub>2</sub>-Al coatings produced by PS and HVOF methods is confirmed by the variation curves of the microhardness distribution (Figure 4), which show a wide range of values between 3250–8650 and 1550–7000 MPa for PS and HVOF, respectively, with two peaks of the most probable microhardness values — 4150 and 6000 MPa for PS (Figure 4, a) and 2450 and 4250 MPa (Figure 4, b) for HVOF. The average microhardness is 5400±1060 MPa for the PS-coating and 3710±950 MPa for the HVOF-coating. The slightly higher microhardness of the PS-coating is evidently associated with a higher content of TiC carbide in the coating, whereas the HVOF-coating contains the softer and more ductile phases of Ti<sub>2</sub>AlC and Ti<sub>3</sub>AlC carbides.

## CONCLUSIONS

The carried out studies have shown that during the MChS process of TiC-TiH<sub>2</sub>-Al powder mixtures, the initial components interact to form the Ti<sub>2</sub>AlC MAX-phase instead of the Ti<sub>3</sub>AlC<sub>2</sub> MAX-phase, for the formation of which the content of the mixture's initial elements had been calculated.

When spraying the TiC-TiH<sub>2</sub>-Al MChS powder system using PS and HVOF methods, a large amount of the initial TiC phase remains in the coatings after spraying, indicating that the reaction between the

components of the MChS powder is not fully completed during spraying.

During the plasma spraying process, the Ti<sub>2</sub>AlC MAX-phase undergoes complete decomposition due to the effect of temperature and interaction with oxygen.

In the HVOF process, the TiC-TiH<sub>2</sub>-Al powder particles do not undergo significant phase transformations and the phase composition of the coating differs only slightly from that of the powder; however, during spraying, partial decomposition of the Ti<sub>2</sub>AlC MAX-phase occurs due to the interaction of the powder particles with oxygen, resulting in the formation of oxides.

During the plasma spraying, coatings are formed with low cohesive strength of the layer, as evidenced by the significant number (11 %) of discontinuities and spalling in the structure. The structure of HVOF-coatings is dense, the coatings are formed of partially melted, deformed particles. The microhardness of the produced PS- and HVOF-coatings is 5.4 and 3.7 GPa, respectively.

## REFERENCE

1. Rahaei, M.B., Jia, D., Rahaei, M., Ghodrati, H. (2017) Manufacturing of high volume fraction of Ti<sub>3</sub>AlC<sub>2</sub>-Ti<sub>2</sub>AlC metallic ceramics as nano-multilayered structures through high energy milling, hot pressing and liquid phase sintering. *Materials Characterization*, **128**, 176–183. DOI: <https://doi.org/10.1016/j.matchar.2017.01.033>
2. Pietzka, M.A., Schuster, J.C. (1994) Summary of constitutional data on the aluminum-carbon-titanium system. *J. Phase Equilib.*, **15**, 392–400. DOI: <https://doi.org/10.1007/BF02647559>
3. Wang, X.H., Zhou, Y.C. (2010) Layered machinable and electrically conductive Ti<sub>2</sub>AlC and Ti<sub>3</sub>AlC<sub>2</sub> ceramics: A review. *J. Mater. Sci. Technol.*, **26**(5), 385–416. DOI: [https://doi.org/10.1016/S1005-0302\(10\)60064-3](https://doi.org/10.1016/S1005-0302(10)60064-3)
4. Zou, Y., Sun, Zh., Tada, Sh., Hashimoto, H. (2007) Rapid synthesis of single-phase Ti<sub>3</sub>AlC<sub>2</sub> through pulse discharge sintering a TiH<sub>2</sub>/Al/TiC powder mixture. *Scripta Material-*

- ia, **56**, 725–728. DOI: <https://doi.org/10.1016/j.scriptamat.2007.01.026>
5. Li, L., Zhou, A., Xu, L. et al. (2013) Synthesis of high pure  $Ti_3AlC_2$  and  $Ti_2AlC$  powders from  $TiH_2$  powders as Ti Source by Tube furnace. *J. of Wuhan University of Technology-Mater. Sci. Ed.*, **28**, 882–887. DOI: <https://doi.org/10.1007/s11595-013-0786-2>
  6. Starostina, A.V., Prikhna, T.A., Sverdun, V.B. et al. (2013) Resistance to high-temperature oxidation of materials based on MAX phases of Ti–Al–(C, N) systems. *Suchasni Problemy Fizychnoho Materialoznavstva*, **22**, 103–107 [in Ukrainian]. <http://www.materials.kiev.ua/article/1821>
  7. Starostina, A.V., Prikhna, T.A., Osadchy A.V., et al. (2011) Investigation of damping properties of materials based on MAX phase  $Ti_3AlC_2$ . *Suchasni Problemy Fizychnoho Materialoznavstva*, **20**, 73–79 [in Ukrainian]. <http://www.materials.kiev.ua/article/2052>
  8. Ivasyshyn, A.D., Ostash, O.P., Prikhna, T.O. et al. (2015) The influence of technological media on mechanical and physical properties of materials for fuel cells. *Fizyko-Khimichna Mehanika Materialiv*, **2**, 7–15 [in Ukrainian].
  9. Zou, Y., Sun, Zh., Hashimoto, H., Cheng, L. (2009) Synthesis reactions for  $Ti_3AlC_2$  through pulse discharge sintering  $TiH_2$ /Al/C powder mixture. *J. of Alloys and Compounds*, **468(1–2)**, 217–221. DOI: <https://doi.org/10.1016/j.jallcom.2008.01.062>
  10. Yang, J., Liao, C., Wang, J., et al. (2014) Reactive synthesis for porous  $Ti_3AlC_2$  ceramics through  $TiH_2$ , Al and graphite powders. *Ceramics Inter.*, **40**, 6739–6745. DOI: <https://doi.org/10.1016/j.ceramint.2013.11.136>
  11. Yang, J., Liao, C., Wang, J. et al. (2014) Effects of the Al content on pore structures of porous  $Ti_3AlC_2$  ceramics by reactive synthesis. *Ceramics Inter.*, **40(3)**, 4643–4648. DOI: <https://doi.org/10.1016/j.ceramint.2013.09.004>
  12. Chen, W., Tang, J., Shi, X. et al. (2020) Synthesis and formation mechanism of high-purity  $Ti_3AlC_2$  powders by microwave sintering. *Inter. J. Appl. Ceram. Technol.*, **17**, 778–789. DOI: <https://doi.org/10.1111/ijac.13452>
  13. Yeh, C.-L., Chen, Y.-T. (2025) Effects of TiC,  $TiH_2$ , Al, and carbon on production of  $Ti_3AlC_2$  by self-sustaining combustion synthesis. *Materials*, **18(6)**, 1293. DOI: <https://doi.org/10.3390/ma18061293>
  14. Shahin, Sh., Kazemi, A. (2016) Mechanochemical synthesis mechanism of  $Ti_3AlC_2$  MAX phase from 5 elemental powders of Ti, Al and C/N. *Advanced Powder Technology*, **27(4)**, 1775–1780. DOI: <https://doi.org/10.1016/j.apt.2016.06.008>
  15. Zhu, J., Gao, J., Yang, J. et al. (2008) Synthesis and microstructure of layered-ternary  $Ti_2AlC$  ceramic by high energy milling and hot pressing. *Materials Sci. and Engineering A*, **490(1–2)**, 62–65. DOI: <https://doi.org/10.1016/j.msea.2008.01.017>
  16. Zakeri, M, Rahimipour, M.R., Sadrnezhad, S.K. (2011) Study on feasibility of  $Ti_3AlC_2$  synthesis by mechanical alloying and heat treatment. *Powder Metallurgy*, **54(3)**, 273–277. DOI: <https://doi.org/10.1179/174329009X457081>
  17. Li, Sh.-B., Zhai, H.-X., Bei, G.-P. et al. (2007) Synthesis and microstructure of  $Ti_3AlC_2$  by mechanically activated sintering of elemental powders. *Ceramics Inter.*, **33(2)**, 169–173. DOI: <https://doi.org/10.1016/j.ceramint.2005.07.024>
  18. Eklund, P., Becker, M., Jansson, U. et al. (2010) The Mn+1AX<sub>n</sub> phases: Materials science and thin-film processing. *Thin Solid Films*, **518(8)**, 1851–1878. DOI: <https://doi.org/10.1016/j.tsf.2009.07.184>
  19. Vihilianska, N., Iantsevitch, C., Olevska, L. et al. (2024) Formation of coatings based on the MAX-phase  $Ti_3SiC_2$  under the conditions of gas-thermal application methods (Overview). *Visnyk KrNU*, **147(4)**, 135–142 [in Ukrainian]. DOI: <https://doi.org/10.32782/1995-0519.2024.4.17>
  20. Zhang, Z., Lim, S. H., Chai, J. et al. (2017) Plasma spray of  $Ti_2AlC$  MAX phase powders: Effects of process parameters on coatings properties. *Surface and Coatings Technology*, **325**, 429–436. DOI: <https://doi.org/10.1016/j.surfcoat.2017.07.006>
  21. Frodelius, J., Sonestedt, M., Björklund, S. et al. (2008)  $Ti_2AlC$  coatings deposited by high velocity oxy-fuel spraying. *Surface and Coatings Technology*, **202(24)**, 5976–5981. DOI: <https://doi.org/10.1016/j.surfcoat.2008.06.184>
  22. Sonestedt, M., Frodelius, J., Palmquist, J.-P. et al. (2010) Microstructure of high velocity oxy-fuel sprayed  $Ti_2AlC$  coatings. *J. of Materials Sci.*, **45(10)**, 2760–2769. DOI: <https://doi.org/10.1007/s10853-010-4263-4>
  23. Yu, H., Suo, X., Gong, Y. et al. (2016)  $Ti_3AlC_2$  coatings deposited by liquid plasma spraying. *Surface and Coatings Technology*, **299**, 123–128. DOI: <https://doi.org/10.1016/j.surfcoat.2016.04.076>

#### ORCID

N.V. Vihilianska: 0000-0001-8576-2095,  
 T.V. Tsymbalista: 0000-0001-9569-7776,  
 O.P. Gryshchenko: 0000-0004-1136-996X,  
 I.O. Koziakov: 0000-0002-0357-9068,  
 O.Y. Gudymenko: 0000-0002-5866-8084

#### CONFLICT OF INTEREST

The Authors declare no conflict of interest

#### CORRESPONDING AUTHOR

N.V. Vihilianska  
 E.O. Paton Electric Welding Institute of the NASU  
 11 Kazymyr Malevych Str., 03150, Kyiv, Ukraine  
 E-mail: [pewinataliya@gmail.com](mailto:pewinataliya@gmail.com)

#### SUGGESTED CITATION

N.V. Vihilianska, T.V. Tsymbalista,  
 O.P. Gryshchenko, I.O. Koziakov, O.Y. Gudymenko  
 (2026) Formation of coatings containing  
 MAX-phases under thermal spraying conditions  
 of TiC– $TiH_2$ –Al powder.  
*The Paton Welding J.*, **05**, 3–9.  
 DOI: <https://doi.org/10.37434/tpwj2026.05.01>

#### JOURNAL HOME PAGE

<https://patonpublishinghouse.com/eng/journals/tpwj>

Received: 25.05.2025

Received in revised form: 24.11.2025

Accepted: 14.05.2026